

Sky coverage assessment for MAORY

C. Plantet^a, G. Agapito^a, L. Busoni^a, M. Bonaglia^a, S. Esposito^a, M. Bellazzini^b, P. Ciliegi^b, S. Oberti^c, M. LeLouarn^c, C. V erinaud^c, and P.-Y. Madec^c

^aINAF, Osservatorio Astronomico di Arcetri, Largo Enrico Fermi 5, 50125 Firenze, Italy

^bINAF Osservatorio Astrofisico e scienza dello Spazio di Bologna (OAS), via Gobetti 93/3
40129 Bologna

^cEuropean Southern Observatory (ESO), Adaptive Optics Department,
Karl-Schwarzschild-Str. 2, D-85748 Garching bei Muenchen, Germany

ABSTRACT

MAORY is the multi-conjugate adaptive optics module for the European ELT. It will provide a >30% Strehl ratio in K-band on the 53x53" field of view of the first-light instrument MICADO. The adaptive optics system itself will consist of 2 post-focal deformable mirrors, 8 laser guide star wavefront sensors and 3 couples of natural guide star wavefront sensors. The latter form the low order and reference module, for fast low-order sensing and slow truth sensing. Both wavefront sensors modules use Shack-Hartmann sensors. In this paper, we present an update on the sky coverage assessment of MAORY. The computation has been refined to take into account the performance on the whole scientific field of view, and the study has been extended to more cases. We show some results that contribute to the main trade-offs of the design: number of deformable mirrors, use of open-loop deformable mirrors in the low-order sensors' path, technical field of view size, low-order sensing strategy... We also evaluate the performance of MAORY on several real fields.

Keywords: Adaptive optics, Wavefront sensing, Multi-Conjugate Adaptive Optics, MAORY

1. INTRODUCTION

MAORY is the Multi-Conjugate Adaptive Optics (MCAO) module for the European ELT.¹ It will provide a >30% Strehl ratio (SR) in K-band on the 53x53" field of view of the first-light instrument MICADO.² The AO system itself will consist of 2 Post-Focal Deformable Mirrors (PFDM), 8 Laser Guide Star (LGS) Wavefront Sensors (WFS) and 3 couples of Natural Guide Star (NGS) WFS. The latter form the LOR (Low Order and Reference) module, for fast low-order sensing and slow truth sensing. Both WFS modules use Shack-Hartmann sensors. We present here the latest results from the sky coverage study. The sky coverage computation itself was previously made considering the on-axis direction only³ but it is now considering the whole MICADO Field of View (FoV). We also have included new C_n^2 profiles derived from recent Stereo-Scidar measurements^{4,5} in the analysis, in order to have a more realistic assessment of the performance. Applying these new features, we pushed further the trade-off study for the main parameters of the system: number of PFDMs, use of open-loop DMs in the LO sensors' path, technical FoV size, LO sensing strategy...). Finally, we applied the sky coverage analysis to a few scientific cases mainly taken from MAORY's white book.

2. SKY COVERAGE ASSESSMENT METHOD

The sky coverage assessment method has already been explained in a previous paper.³ The only difference here is that we compute the residuals not only on axis, but also in different directions of the scientific FoV in order to average the residuals or the SR. We quickly recall here the considered error budget terms and how they are computed:

Further author information:

C.P.: E-mail: cedric.plantet@inaf.it, Telephone: +39 0552752289

- Tomographic error: this error is due to the anisoplanatic nature of the turbulence and depends on the NGS asterism geometry. It is computed using analytical formulas of the covariance of Zernike modes from 2 different sources.⁶
- Noise error: we propagate the noise on each NGSWFS (derived from a series of end-to-end simulations considering different NGS magnitudes and positions) through the low-order tomographic reconstruction.
- Windshake: we apply a temporal filter of order 2 on the windshake tip/tilt Power Spectral Densities (PSD) while considering a certain level of noise (derived from WCoG measurements error for a given SR and magnitude), in a SCAO-like manner. Indeed, the windshake tip/tilt is isoplanatic and can be measured on the brightest available star only. The temporal filter is optimized for each noise level in terms of poles, zeros and gain, the frequency being fixed at 500 Hz.

To these low order terms, we add the high orders (HO) from end-to-end simulations and a fixed error part to take into account NCPAs, LGS elongation, telescope aberrations. . . This fixed part is taken from other studies in the framework of MAORY and amounts to 145 nm.

In the following, all sky coverages are computed at the South Galactic Pole.

3. CN2 PROFILES

A new database of C_n^2 measurements from a Stereo-Scidar at Paranal was recently released.^{4,5} It contains more than 10,000 profiles measured over 2 years. These profiles can be used to have a better assessment of MAORY's performance. However, running end-to-end simulations on this many profiles is not feasible with standard hardware. We thus thought of a way of classifying them with a given figure of merit and derive a few profiles that would be representative of different turbulence conditions.

The best figure of merit to classify the profiles is the residual we get from each profile, that can be quickly computed with a Fourier analysis.⁷ However, these residuals are dependent on the system configuration (number of PFDMs, pitch, number of LGSs. . .). We looked for a correlation between the residuals and a parameter that would be only turbulence-dependent and found the figure of merit $seeing/\theta_0$, with θ_0 the isoplanatic angle. Though this criterion does not seem to have any physical meaning, we found that it is significantly correlated to the performance for any configuration (Fig. 1). Indeed, the lower this ratio, the better the turbulence conditions, hence the better the performance for any tomographic AO system.

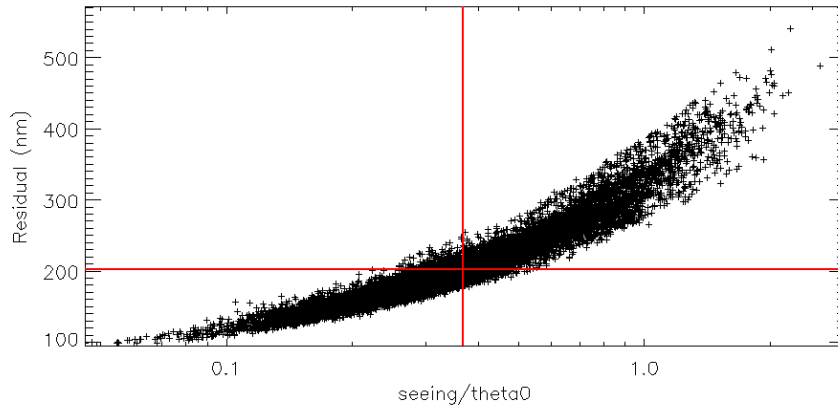


Figure 1. On-axis residual given by a Fourier analysis for each of the 10,000 profiles as a function of the $seeing/\theta_0$ ratio. Configuration: 2 PFDMs with pitches 1.5m and 1.7m (700 actuators each) respectively conjugated at 8 km and 16 km, 6 LGSs at 45". The red lines correspond to the median residual and the median $seeing/\theta_0$.

We selected 5 single profiles out of the 10,000 that corresponds to percentiles of 10%, 25%, 50%, 75% and 90%. Here, we mean by percentile the probability to have a given $seeing/\theta_0$ or lower, so the 50% profile actually

corresponds to the median and it will be the profile we will use in the rest of the paper. This profile is plotted in Fig. 2.

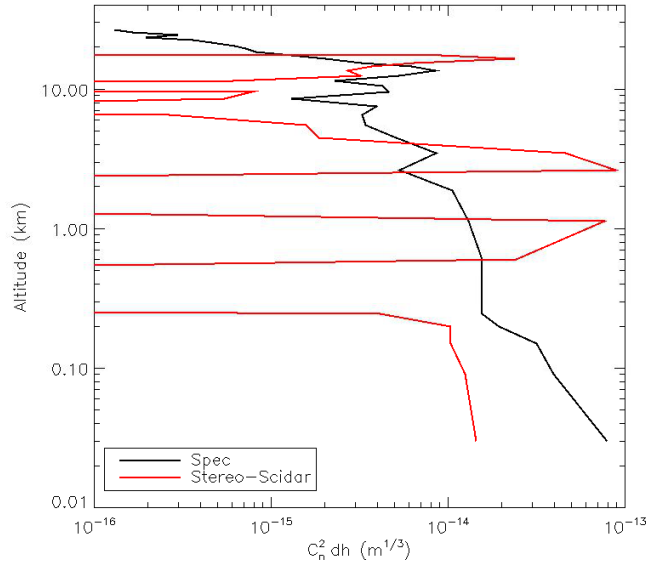


Figure 2. C_n^2 profile for the 50% percentile (in red). The median profile from the E-ELT specifications is also plotted (in black) for reference.

4. TRADE-OFF STUDY

In this section, we present some aspects of the trade-off study in the light of this new median profile we have decided to use and of the more accurate sky coverage computation. We focus here on the number of low orders to be estimated, the technical FoV size, the number of PFDMs, the number and positions of the LGSs and the use of an open-loop DM in the LO sensor path (so-called Dual AO⁸). In the following, the first PFDM is conjugated at 16 km and the second at 8 km.

4.1 Number of estimated LO modes

The LO Shack-Hartmann sensors have 2×2 subapertures, meaning that they can measure modes up to astigmatism, which was the chosen strategy until now. However, the estimation of focus and astigmatism suffers a lot from tomographic and noise error when we are dealing with a bad NGS asterism. By estimating them on the LGSs, we would gain on both these errors since the LGSs are bright and closer to the optical axis. Of course, the focus estimation would be biased due to the altitude variation of the sodium layer, but we can correct it slowly with the measurements of the NGSWFSs. Fig. 3 shows the important gain we get just by changing the number of modes, the number of subapertures still being 2×2 . Even at 0% sky coverage, we gain a few points of SR because the estimation on the LGSs is still better than on the best possible NGS asterism. The residual of the sodium focus correction is of course added to the tip/tilt only curve. It amounts to 35 nm and has been computed from a temporal filtering of the sodium altitude variation PSD ($= \alpha \nu^\beta$ with $\alpha = 31 m^2/Hz$, $\beta = -1.95$ and ν the temporal frequency⁹) considering sensors running at 10 Hz.

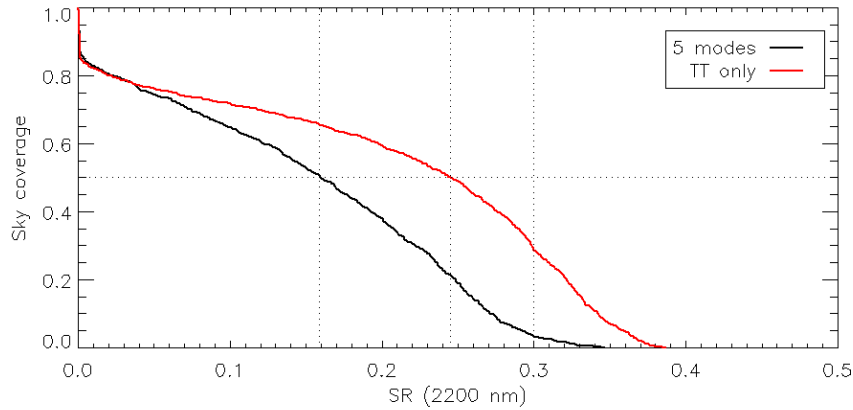


Figure 3. Sky coverage vs. SR in K for LO sensors measuring 5 modes (black) or tip/tilt only (red). Configuration: 1 PFD with 700 actuators, 6 LGSs at 45". An additional 35 nm is added to the red curve to take into account the residual focus from the sodium altitude variation.

There is thus a clear advantage in estimating only tip/tilt with the LO sensors, which is now the current strategy. Since we are not estimating focus and astigmatism anymore, we could use a full aperture image to measure tip/tilt and gain in signal-to-noise ratio. However, this means that we would have to measure the focus at a frequency greater or equal to 10 Hz on the reference sensors to avoid a significant residual from the sodium variation. This would strongly limit the sky coverage, hence we decided to keep the 2×2 configuration which allows a sufficiently fast sensing of focus.

4.2 Technical FoV size

In order to ensure a good sky coverage, one would like to have a technical FoV as large as possible. Though, a large technical FoV also means a more complex opto-mechanical design and a better sky coverage is not always guaranteed since further stars have a poor signal-to-noise ratio.

The baseline technical FoV diameter was 180" until now. We had previously found that going to a larger FoV would not provide a significant improvement on sky coverage. On the contrary, reducing it might lower a sky coverage a bit with the compensation of a better optical design (i. e. less NCPAs, less distortion, increased feasibility of the whole system...). In Fig. 4, we show that a 160" diameter technical FoV would provide a sky coverage close to the 180" technical FoV. The impact of having a more compact optical system has not been clearly evaluated yet but the loss of SR was deemed fine with respect to the overall system simplification.

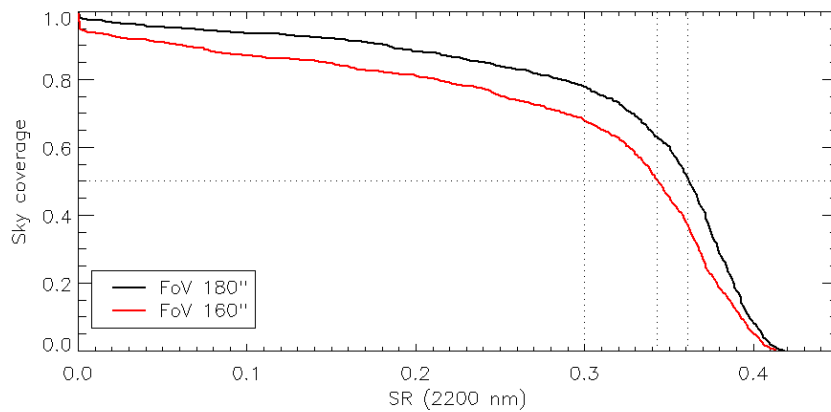


Figure 4. Sky coverage for a technical FoV diameter of 180" (black) or 160" (red). Configuration: 2 PFDs with 700 actuators and 6 LGSs.

4.3 Number and positions of the LGSs

The number and positions of the LGSs directly impacts the tomographic error for the HOs and thus indirectly impacts the performance of the LO sensors, as they might see a different SR on the NGSs. There is a trade-off to be made between LGSs close to the center, providing a good correction in the scientific FoV but a low correction on the NGSs, and LGSs far off-axis, providing the opposite. It is also interesting to see whether adding more LGSs provide a significant gain on sky coverage or not. In Fig. 5, we compare different configurations from 6 to 12 LGSs with fine pitch PFDMs (4000 actuators) in order not to be limited by their fitting error. We find that having 8 LGSs instead of 6 adds a few points of SR, the best geometry being on two rings at 45" and 60". More LGSs would not improve the performance: 8 LGSs do as well as 12 LGSs in the same configuration.

The new baseline is thus 8 LGSs, though it is not sure that the telescope will be able to provide more than 6 LGSs. In the following, we continue considering 6 LGSs to remain conservative.

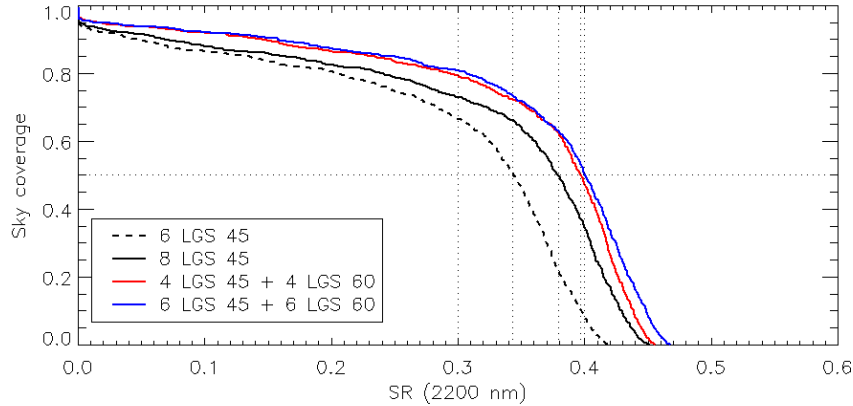


Figure 5. Sky coverage for different LGS asterisms: 6 or 8 LGSs at 45", 4 LGSs at 45" and 4 at 60", 6 LGSs at 45" and 6 LGSs at 60". Configuration: 2 PFDMs with 4000 actuators.

4.4 Number of DMs and Dual AO

Finally, we investigate the number of PFDMs and the possibility to add an open-loop DM in the path of the LO sensors (Dual AO). The goal of the latter would be to improve the SR of the NGS in case it is not well corrected. The Dual AO would have a meaning in a system with 1 PFDM, to compensate for the fact that we do not have a second PFDM that would increase the correction level in the technical FoV. The advantage with respect to having 2 PFDMs would mostly be the cost. In Fig. 6, we compare the sky coverage for 1 PFDM, 1 PFDM with a Dual AO correcting 500 modes and 2 PFDMs. A third PFDM would clearly be out of the allocated budget, so we do not consider it. We see that the performance of the 1 PFDM + Dual AO configuration is at the midpoint between 1 PFDM and 2 PFDMs, whatever the PFDM pitch. It is then preferable to keep 2 PFDMs.

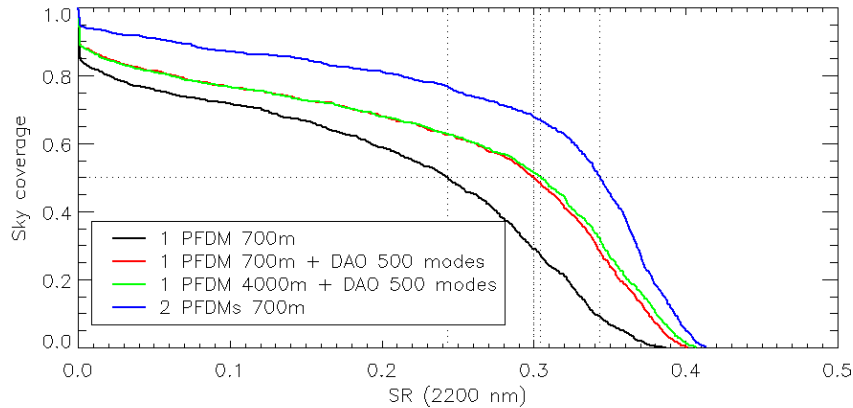


Figure 6. Sky coverage for 1 PFDM alone or with a Dual AO correcting 500 modes and for 2 PFDMs. Configuration: 6 LGSs at 45".

5. SCIENTIFIC CASES

We apply the sky coverage computation to 3 science cases for MAORY. Here the computation is based on real star catalogs. The first science case actually relies on the sky coverage of MAORY, as only a few stars are available around the targets (the number of available NGSs might be pessimistic with current catalogs since they have a low limiting magnitude), while the 2 other ones are in the Large Magellanic Cloud (LMC), where plenty of bright stars can be selected. For these 2 cases, we are mostly interested in the statistics of the performance in the pointed region.

In the following, we always consider a system with 2 700-actuator PFDMs and 6 LGSs at 45".

5.1 High redshift galaxies

The first science case aims to study the central region of galaxies at a redshift $z > 1.5$, in order to confirm the relationship between the central mass density and the star formation rate. 22 targets have been selected from the UltraVISTA catalog.¹⁰ The desired SR is 50% in K. This goal is optimistic: even with the best possible configuration, we have a SR at 0% sky coverage lower than 50%.

We plot in Fig. 7 the SR obtained for each of the targets. 3 of them were discarded as no star was available within the technical FoV. We find that 10 of the targets have a $SR \gtrsim 30\%$, which is relatively good since MAORY's requirement is 30% of SR with 50% sky coverage assuming the specification median C_n^2 profile, which has a larger θ_0 .

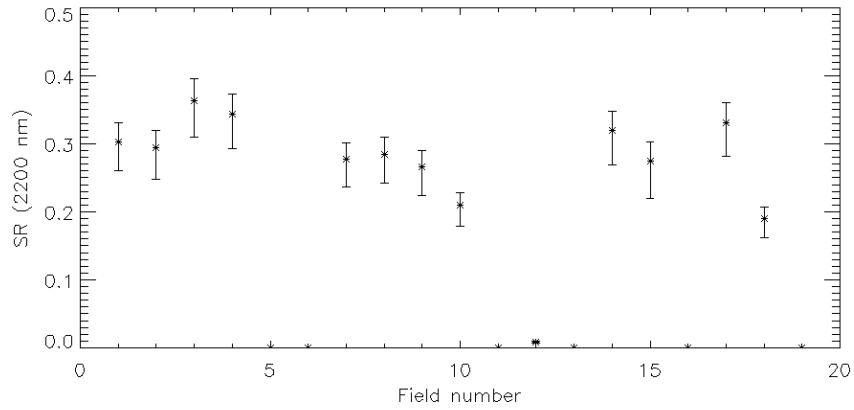
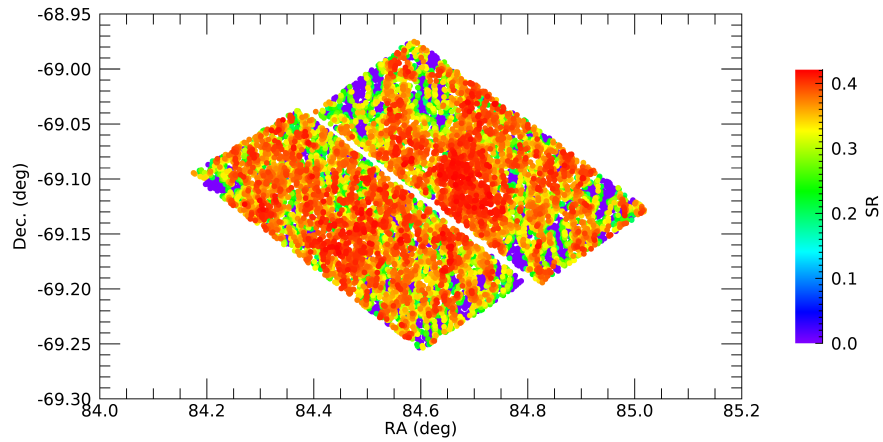


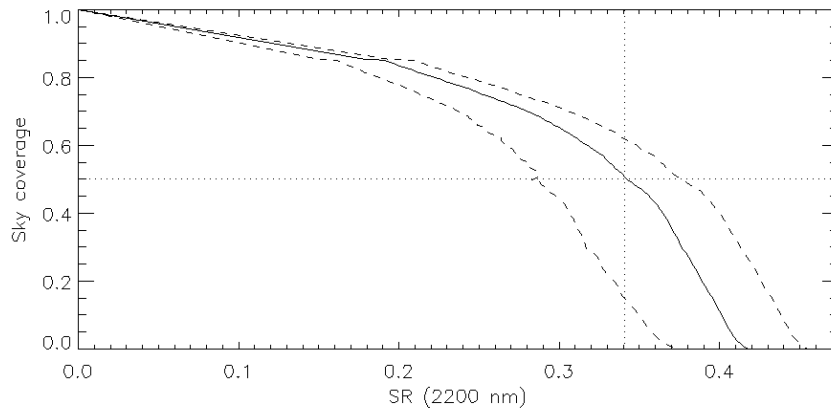
Figure 7. SR for each target of the first science case (UltraVISTA catalog). The error bars give the minimum and maximum SR in the scientific FoV.

5.2 Tarantula nebula

The second case is a study of the stellar population and dynamics in the Tarantula nebula, in the LMC. The star catalog used here is HTTP,¹¹ with some inputs from 2MASS.¹² A map of the SR and the SR statistics are shown in Fig. 8. The performance is again satisfying, with a 34% median SR and a good PSF uniformity (less than 10% difference between the minimum SR and the maximum SR in the scientific FoV). Note that the magnitude has been limited to $H = 14$ to avoid time-consuming computations as they are many stars. Hence, the result is slightly pessimistic.



(a) SR map

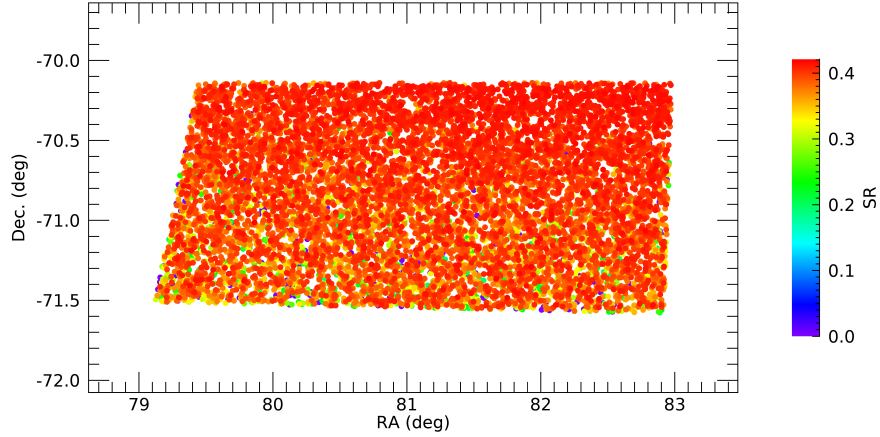


(b) SR statistics

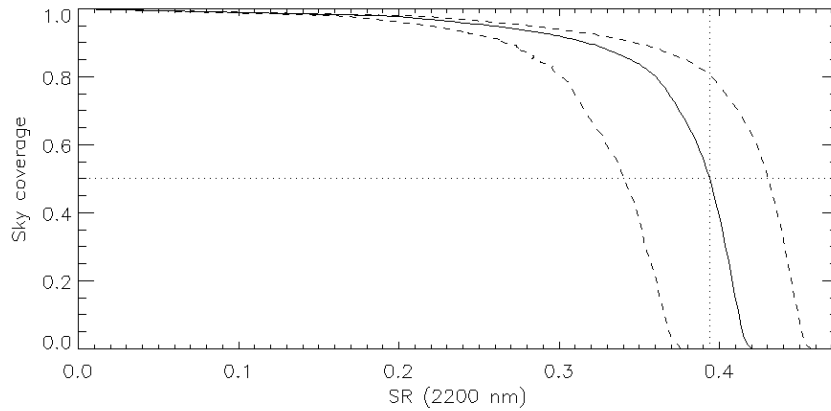
Figure 8. Top: SR map for the Tarantula nebula science case. Bottom: Statistics of the SR. Dashed lines correspond to the minimum and maximum SR in the scientific FoV.

5.3 VMC survey

This last case is actually not part of MAORY’s white book. We just use the recently completed VMC survey¹³ to get an assessment of performance in a region that could be of interest for astronomers. We ran the sky coverage analysis on the tile LMC 5_5, close to the LMC’s galactic center. Again, we had to limit the magnitude (to $H = 15$) to avoid time-consuming computations. A map of the SR and the SR statistics are shown in Fig. 9. The median SR is 39% and in 80% of cases we have a $SR > 35\%$ with a uniform PSF in the scientific FoV.



(a) SR map



(b) SR statistics

Figure 9. Top: SR map for the VMC science case. Bottom: Statistics of the SR. Dashed lines correspond to the minimum and maximum SR in the scientific FoV.

6. CONCLUSION

We have presented new results for the sky coverage of MAORY. The computation has been made more realistic by considering the whole MICADO FoV and by using a C_n^2 profile from recent stereo-scidar measurements at Paranal.

We have performed the sky coverage analysis with different system configurations in order to do the main trade-offs. We have then upgraded our LO sensing strategy, from 5 estimated modes to tip/tilt only, evaluated the impact of reducing the technical FoV for a better optical design, shown that 2 additional LGSs were sufficient to optimize our tomographic reconstruction and confirmed the need for a second PFDM.

Finally, we assessed MAORY's performance for a few science cases. In crowded fields, we easily reach a SR between 35% and 40% in K. When dealing with deep-sky objects, MAORY gives a SR of approximately 30% or higher in almost 50% of the cases. These results are satisfying as they are close to the initial objectives of MAORY.

ACKNOWLEDGMENTS

The first author acknowledges INAF contract 11 (DD n. 27/2016) for financial support.

REFERENCES

- [1] Diolaiti, E. et al., “MAORY: adaptive optics module for the E-ELT,” *SPIE Proceedings* (2016).
- [2] Davies, R. et al., “MICADO: first-light imager for the E-ELT,” *SPIE Proceedings* (2016).
- [3] Plantet, C., Agapito, G., Giordano, C., Busoni, L., Bonaglia, M., Esposito, S., Arcidiacono, C., Cortecchia, F., Ciliegi, P., Diolaiti, E., Bellazzini, M., Ragazzoni, R., and Feautrier, P., “LO WFS of MAORY: performance and sky coverage assessment,” in [*Adaptive Optics Systems VI*], Close, L. M., Schreiber, L., and Schmidt, D., eds., **10703**, 1141 – 1154, International Society for Optics and Photonics, SPIE (2018).
- [4] Osborn, J., Wilson, R. W., Butterley, T., Morris, T. J., Dubbeldam, M. F., D erie, F., and Sarazin, M., “E-ELT turbulence profiling with stereo-SCIDAR at Paranal,” in [*Astronomical Telescopes + Instrumentation*], (2016).
- [5] Sarazin, M. S., Osborn, J., Chacon-Oelckers, A., Drie, F. J., Louarn, M. L., Milli, J., Navarrete, J., and Wilson, R. R. W., “Preliminary results from the Stereo-SCIDAR at the VLT Observatory: extraction of reference atmospheric turbulence profiles for E-ELT adaptive optics instrument performance simulations,” in [*Optics in Atmospheric Propagation and Adaptive Systems XX*], Stein, K. U. and Gladysz, S., eds., **10425**, 79 – 88, International Society for Optics and Photonics, SPIE (2017).
- [6] Whiteley, M. R., Roggemann, M. C., and Welsh, B. M., “Temporal properties of the Zernike expansion coefficients of turbulence-induced phase aberrations for aperture and source motion,” *J. Opt. Soc. Am. A* **15**, 993–1005 (Apr 1998).
- [7] Neichel, B., Fusco, T., and Conan, J.-M., “Tomographic reconstruction for wide-field adaptive optics systems: Fourier domain analysis and fundamental limitations,” *JOSA A* **26**(1), 219–235 (2009).
- [8] Rigaut, F. and Gendron, E., “Laser guide star in adaptive optics-The tilt determination problem,” *Astronomy and Astrophysics* **261**, 677–684 (1992).
- [9] Pfrommer, T. and Hickson, P., “High-resolution lidar observations of mesospheric sodium and implications for adaptive optics,” *J. Opt. Soc. Am. A* **27**, A97–A105 (Nov 2010).
- [10] McCracken, H., Milvang-Jensen, B., Dunlop, J., Franx, M., Fynbo, J., Le F evre, O., Holt, J., Caputi, K., Goranova, Y., Buitrago, F., et al., “UltraVISTA: a new ultra-deep near-infrared survey in COSMOS,” *Astronomy & Astrophysics* **544**, A156 (2012).
- [11] Sabbi, E., Lennon, D., Anderson, J., Cignoni, M., Van Der Marel, R., Zaritsky, D., De Marchi, G., Panagia, N., Gouliermis, D., Grebel, E., et al., “Hubble tarantula treasury project. III. Photometric catalog and resulting constraints on the progression of star formation in the 30 Doradus region,” *The Astrophysical Journal Supplement Series* **222**(1), 11 (2016).
- [12] Skrutskie, M., Cutri, R., Stiening, R., Weinberg, M., Schneider, S., Carpenter, J., Beichman, C., Capps, R., Chester, T., Elias, J., et al., “The two micron all sky survey (2MASS),” *The Astronomical Journal* **131**(2), 1163 (2006).
- [13] Cioni, M.-R., Clementini, G., Girardi, L., Guandalini, R., Gullieuszik, M., Miszalski, B., Moretti, M.-I., Ripepi, V., Rubele, S., Bagheri, G., et al., “The VMC survey-I. Strategy and first data,” *Astronomy & Astrophysics* **527**, A116 (2011).